Scientific Reviews
&
Chemical Communications

*Sci. Revs. Chem. Commun.: 6(4), 2016, 63-83*
*ISSN 2277-2669*

# WATER RESISTANT FLUORINE-FREE TECHNOLOGIES FOR SYNTHETIC FABRICS

**NIKOLAY BARASHKOV[a*], TAMARA SAKHNO[b], ANATOLIY SEMENOV[b], IRINA IRGIBAYEVA[c] and YURIY SAKHNO[d]**

[a]Micro-Tracers, Inc, San Francisco, CA, USA
[b]University of Economics and Trade, POLTAVA, UKRAINE
[c]Eurasian National University, ASTANA, KAZAKHSTAN
[d]L' Institut des Matériaux de Paris Centre, PARIS, FRANCE

(*Received : 26.09.2016; Revised : 23.10.2016; Accepted : 26.10.2016*)

## ABSTRACT

The authors pointed out the disadvantages of well known poly(fluoroalkyl acrylate) coatings that were broadly used in the past for providing a water repellency for rainwear. It was found that hydrophobic organic-inorganic hybrid materials described by the authors of this article provide a beneficial alternative to poly(fluoroalkyl acrylates) due to their environmentally and toxicologically friendly nature. Several basic approaches to improved hydrophobicity and superhydrophobicity are considered and their applicability for enhancing hydrophobic properties of polyester and polyamide fibers is analyzed. The prospects of using titanium-based precursors and organic silanes in sol-gel processes appear to be most realistic in terms of practical application.

**Key words**: Hydrophobicity, Hybrid materials, Self-cleaning coatings, Sol-gel method, Titanium-based precursor, Functional silanes.

## INTRODUCTION

### Hybrid materials with improved hydrophobicity

Water repellency for rainwear has historically been achieved through the use of poly(fluoroalkyl acrylate) coatings. These coating materials are highly effective at repelling water and durable, however, long chain versions of these coatings are being phased out due to environmental and toxicological concerns. Of greatest concern are the "C8" fluoroacrylate based materials, which can contain perfluorooctanoic acid (PFOA). PFOA is persistent and mobile in the atmosphere and aqueous environments, due to its chemical stability and low volatility. Animal toxicology studies performed with PFOA indicate potential developmental, reproductive and systematic effects. After oral exposure, PFOA accumulates and adsorbs in the serum, kidney, and liver. This compound is resistant to direct oxidation, photolytic degradation, biodegradation and air stripping/vapor extraction, making their removal difficult. These are the main reasons why the textile industry is currently undergoing a transition away from these "C8" materials[1]. On the other hand, hydrophobic organic-inorganic hybrid materials attracted significant attention recently due to their

Available online at www.sadgurupublications.com
*Author for correspondence; E-mail: Nikolay@microtracers.com

ability to be produced in large scale[1,2]. Such numerous areas of application, as non-stick and self-cleaning coatings, anti-stain coating, flexible substrate fabrication, semi-conducting channels, cell adhesion and transporting, drug delivery, micro-patterning, photovoltaic applications, as well as several others are taking advantages from using multi-functional hybrid materials[1-3]. Several types of synthetic procedures, including sol-gel method, based on using functional silanes and other functional precursors have been proposed and successfully tested for preparation of multi-functional hybrid materials[4-6].

The large varieties of stable hybrid substrates presented by powders, fibers, foams, flexible films and monoliths have been processed by extrusion, spin coating, casting, spraying, dip-coating and several other means[7]. A number of polymerization techniques, particularly emulsion polymerization, controlled/living radical polymerization and surface initiated atom transfer radical polymerization were implemented for synthesis of multi-functional hybrid materials[4,5,20,21]. Keeping in mind that the main subject of current overview is the hybrid materials with improved hydrophobicity it should be emphasized that depending of functional groups in these materials they can display hydrophilic surface properties (contact angle (CA) < 90°), hydrophobic properties (CA ≥ 90°) or superhydrophobic surface properties (CA ≥ 150°)[8-10,28]. Moreover it was reported[11,12,17] that the hybrid materials can be switchable, i.e. their surface properties could be hydrophobic or hydrophilic. The changes in the surface nature may be triggered by stimuli such as temperature, pH, UV-light exposure and alike. Organic-inorganic hybrid materials used for fabrication of hydrophobic and superhydrophobic surfaces attracted significant attention in many applications within last 15-20 years (Fig. 1).

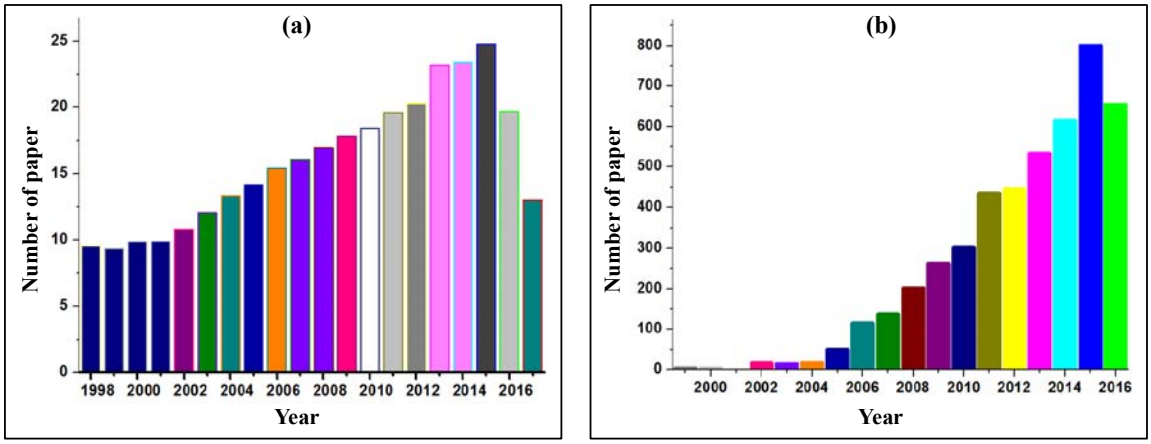


**Fig. 1: Number of papers published in ten years 1998-2016 under the topic of (a) hydrophobic/or hydrophobicity and (b) superhydrophobic/or superhydrophobicity**

The comprehensive review of publication in the area of various organic-inorganic hybrid materials and their development has been provided relatively recently[12]. Such polymers as Polymethylhydrosiloxane (PMHS), poly(vinyl chloride) (PVC), fluorinated methacrylate and mercapto functional monomers, various functional silane precursors, lotus leaf (*Nelumbo nucifera*, LL) and tree of heaven leaf (*Ailanthus altissima*, TL) powder have been succesfully used for hydrophobic and superhydrophobic surface fabrication[3,13]. PMHS is a well known siloxane component with high softness, solubility in common organic solvents, non-toxicity, inertness to air and moisture, low surface energy, hydrophobicity and thermally stable properties[3,14]. PMHS was used in various applications such as reducing agent for organic synthesis, fabrication of stable hydrophobic and superhydrophobic surfaces, coatings on glass, micro-fluidic chips, electronic packages, actuators, and optical fibers[3,14,15]. On the other hand, PVC is the most widely used polymer in electronic applications due to the excellent electrical insulation property, inherent flame-retardance, weathering stability, process ability, energy recovery and recyclability[8]. Various silane precursors, fluorinated

methacrylate, and mercapto functional monomer were used to enhance the properties of PMHS and PVC in the hybrid systems[8]. Recently, novel bio-inspired hybrid micro-nano composites by the use of LL powder, PMHS, and functional silica ormosils have been developed[9,13,16]. The obtained hybrid suspension showed highly stable superhydrophobicity on any substrate by simply drying the solvent at room temperature for a few minutes. The hybrid loaded melamine sponge showed selective oil absorption from the oil spill on the water surface. Moreover the superhydrophobic sponge can also absorb various organic solvents and can be recycled for several times for the absorption of larger amounts of oils and organic solvents on the water surface or in under-water.

The practical applications of these hybrid materials and related scale up experience will be discussed in details in section 2. However, before going to these details, it is appropriate to consider some basics of the theory of superhydrophobicity.

**Theory of superhydrophobicity**

According to[17], the underlying theories interpreting the wetting phenomena are mainly focused on Young's equation, Wenzel equation, and Cassie–Baxter equation, despite the fact that the wetting phenomena have been studied over the past decades. Based on these theories, scientists have understood that both surface chemical composition and its morphology can influence the contact angle of liquid droplets on solid surfaces. However, such equations are not sufficient to thoroughly explain the mechanisms of wetting phenomena, although they are still necessary. The authors of study[17] reviewed the theory from the classical wetting models to the most recent theoretical advances of superhydrophobic surfaces with regard to the wetting process.

As it was stated earlier, generally, a superhydrophobic surface is defined as having a water contact angle (CA) greater than 150° but a slide angle (SA) less than 5°.[18] Such a surface already exists commonly in the biological world, especially exhibited by lotus leaf, that is, the so-called lotus effect. Many plant leaves and specific surfaces of animals in nature all exhibit this so-called lotus effect, where the interplay of surface microstructure and chemical composition causes water droplets to remain spherical on the surface. It is usually believed that wettability is a tendency for a liquid to spread on a solid substrate and is generally characterized by the CA, which is defined geometrically as the angle formed by a liquid at the three phase boundary where a liquid, gas and solid intersect each other as shown in Fig. 2. It is one of the most important properties that can be employed to assess the hydrophobic capability of surface, and has a significant influence on agriculture, industries and daily life[17].

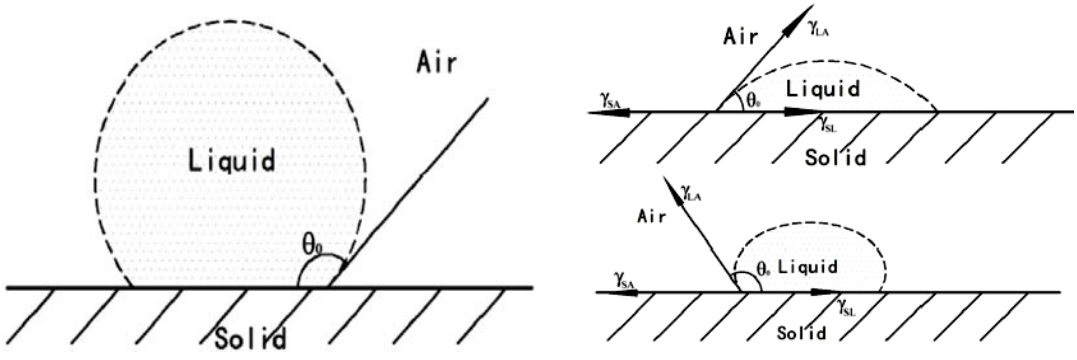


**(a)** **(b)**

**Fig. 2: (a) Liquid droplet on a flat substrate; (b) A sketch map showing a simple derivation of Young's equation using surface tension vectors for a liquid on a solid substrate**[17]

Furthermore, it is confirmed by researchers all over the world that the wetting behavior of a liquid on a solid surface depends not only on the chemical composition but also on the morphological structure[19]. Thus attention on this research filed is mainly paid to two following aspects. On the one hand, systematic detailed thermodynamic analyses on free energy and free energy barrier have been investigated for the purpose of reducing the surface free energy. On the other hand, researchers found that micro- and nanostructures play a key role in the wetting of surface, regardless of chemical composition on the basis of the established theoretical models and experimental results.

Several geometrical models, including Wenzel model[20], Cassie-Baxter model[21], composite structure with double- scale cylindrical groove model[22], a model with paraboloids of revolution[23] have been developed for better understanding of the mechanism of superhydrophobic surfaces and further guide the design and fabrication of biomimetic superhydrophobic surfaces. Although these theoretical models proposed have been used to elucidate the principles of superhydrophobic surfaces, they are suitable only for specific conditions and still contain a lot of experiential parameters. Therefore, they don't have the universal applicability for all superhydrophobic states except improving these models before being used. In opinion of the authors of overview[17], it would be desirable to establish the typical theories and models with widespread applicability to explain the relationships between structures and properties quantitatively.

**Basic theories: Contact angle and Young's equation**

The CA of liquid on a solid surface is an important parameter for characterizing the surface wettability and predicting its wetting behavior in practical applications. Therefore, the value of water CA on a surface can be used for determining its hydrophobicity, denoting a surface with its CA below 90° as hydrophilicity. On the basis of this definition and the deep investigation of surfaces, the wetting behavior of surface can be subdivided two classes: one on which CA is between 90° and 150° can be denoted as a hydrophobic surface, but the other proposed afterward, a surface where CA is above 150°, is denoted as a superhydrophobic surface. In terms of a superhydrophobic surface, the other important limited condition is a low CA hysteresis which is usually below 5°.

The definitions stated above are both based on the ideal smooth surface without fully considering the effect of surface morphology and other factors. Given their potential applications of wetting/nonwetting surfaces, it is desirable to construct the rational theoretical models for explaining the mechanism and establishing the quantitative equations to predict the wetting behavior of a surface. Since 1805 it was proposed that an interface between two materials had specific energy, the so-called interfacial energy, which is proportional to the interfacial area[17]. This concept has laid foundation for the field of wettability, which has become a very popular topic in the last two decades, thanks to biological and high-technology applications ranging from self- cleaning surfaces, microelectronics and thin film coatings, to image formation that involves the spreading of liquids on solid surfaces.

It is well known that the surface atoms or molecules of liquids or solids have higher energy than similar atoms and molecules in the interior, which results in surface tension or surface free energy so as to reach stable state with relatively lower energy. As a rule, the surface tension or free surface energy can be used to evaluate the surface property quantitatively. Its value is equal to the surface work which is required to create per unit area of the surface at constant volume and temperature. The units of $\gamma$ are $J/m^2$ or N/m and it can be interpreted either as energy per unit surface area or as tension force per unit length of a contact line at the surface. When a solid (S) is in contact with liquid (L), the molecular attraction will reduce the energy of the system so as to reach a equilibrium value which is less than the sum of two separated surfaces. The formation or establishment of interface during the wetting process is governed by thermodynamic principle of energy reduction. The elimination of two surfaces to form an interface reduces the total energy of system.

Hence, the thermodynamic condition for wetting to occur can be written as[24]:

$$\gamma_{SA} \geq \gamma_{SL} \geq \gamma_{LA}$$

where $\gamma_{SA}$ and $\gamma_{LA}$ are the surface energies (surface tensions) of the solid and liquid against air, and $\gamma_{SL}$ is the interface energy (interface tension) between solid and liquid. Then the work of adhesion may be expressed by the Dupré equation:

$$W_{SL} = \gamma_{SA} + \gamma_{LA} - \gamma_{SL} \quad \ldots(1)$$

In this equation, WSL is the work of adhesion per unit area between two surfaces.

If a droplet of liquid is placed on a solid surface, the liquid and solid surfaces come together under equilibrium at a characteristic angle called the static CA $\theta_0$ (Fig. 2). The CA can be determined by the condition of the total energy of the system being minimized[25].

The total energy $E_{tot}$ is given by equation (2)[26]:

$$E_{tot} = \gamma_{LA} (A_{LA} + A_{SL}) - W_{SL}A_{SL} \quad \ldots(2)$$

Where $A_{LA}$ and $A_{SL}$ are the contact areas of liquid-air and solid-air interface, respectively. It is assumed that the droplet is small enough so that the gravitational potential energy can be neglected.

At the equilibrium $dE_{tot} = 0$, this yields

$$\gamma_{LA} (dA_{LA} + dA_{SL}) - W_{SL}dA_{SL} = 0 \quad \ldots(3)$$

For a droplet of constant volume, it is easy to show from geometrical considerations that –

$$\frac{dA_{LA}}{dA_{SL}} = \cos\theta_0 \quad \ldots(4)$$

Therefore, the so-called Young's equation for the CA is obtained as follow according to Eqs. 1, 3 and 4.

$$\cos\theta_0 = \frac{\gamma_{SA} - \gamma_{SL}}{\gamma_{LA}} = \frac{W_{SL}}{\gamma_{LA}} - 1 \quad \ldots(5)$$

or

$$\gamma_{SL} = \gamma_{SA} - \gamma_{LA} \cos\theta_0 \quad \ldots(6)$$

It is can be seen that eqs. 5 and 6 provide the value of the static CA for given surface tensions[26].

Young's equation is using surface tension vectors for a liquid on a solid substrate. In fact, for an ideal solid surface, the influences of roughness, chemical heterogeneity, surface reconstruction, swelling and dissolution are neglected. Complete wetting state corresponds to $\theta_0 = 0$, and typically happens for liquids with low surface tension $\gamma_{LA}$, and on solids with high surface energy $\gamma_{SA}$.

For $\gamma_{SA} > \gamma_{SL}$ then $0^o < \theta_0 < 90^o$ and for $\gamma_{SA} < \gamma_{SL}$ then $90^o < \theta_0 < 180^o$. According to the Young's equation, it is clear that the interfacial tension between the solid and liquid $\gamma_{SL}$ is lower than $\gamma_{SA}$ only when $\theta_0 < 90^o$, this happens only in the case of wetting. But $\gamma_{SL} > \gamma_{SA}$ can happen only when $\theta_0 > 90^o$, the contact area of the liquid-solid interface will be reduced. In this case the liquid behaves as non-wetting because $\gamma_{LA}$ is always finite and positive value, then to minimize the total surface/interfacial energy of the liquid.

Thus the CA depends on the optimization of the contact area of the solid-liquid and the liquid-air interface. More importantly, the wetting property of a liquid on a flat solid substrate can be also understood from the thermodynamics of surfaces by evaluating the work of adhesion, thus leading to Young's equation. Another simple derivation of Young's equation can be obtained by balancing the forces at the line of contact where all of the three medium (solid, liquid and vapor) meet together as shown schematically in Fig. 2B.

Thus, the equilibrium CA of the liquid drop upon the smooth and flat substrate depends on the value of the difference between $\gamma_{SA}$ and $\gamma_{SL}$ as expressed above. It is inferred that liquids with high surface tension on surfaces with low surface energy tend to form droplets with high CA. Eqs. 5 and 6 are deduced under condition that the substrate 5 is assumed to be perfectly smooth, homogeneous, and rigid. However, there are no absolute smooth ideal surfaces, structured or rough surfaces exist commonly in reality. So the authors of overview[17] concluded that it's necessary to know how the CA functions on a rough surface.

**Wenzel model**

This model firstly introduced the concept of surface roughness into the theoretical study on wetting behavior almost 80 years ago[20]. According to this model, it was necessary to modify the Young's equation based on the comprehensive considerations of the influence of roughness on wettability. Since then, when one considered the wetting behavior of a liquid droplet deposited on a rough solid surface, the Wenzel model[20] can be used as the analytical model to quantitatively evaluate the wetting/non-wetting. Recently, more and more experimental results have indicated that the roughness of a solid surface can greatly magnify the wetting property of the solid even without taking account of chemical composition.

As forces are more easily visualized than energy values, it is conventional, in the analysis of wetting problems, to define force concepts (the interfacial surface tensions) as ones numerically equal to the characteristic interfacial specific energy values, and to deal with these forces as vector quantities constant in magnitude and variable in direction. It is in this translation from energies to forces that the importance of the physical condition of solid surfaces is likely to be obscured. Then a distinction between the total or "actual surface" and the superficial or "geometric surface" of an interface should be recognized. The latter is the surface as measured in the plane of the interface. Perfect smoothness is an acceptable assumption, where actual surface and geometric surface are identical, but at the surface of any real solid the actual surface will be greater than the geometric surface because of surface roughness. This surface ratio is termed the "roughness factor" and designated by $r$[20]:

$$\text{r} = \text{Roughness factor} = \frac{\text{Actual surface}}{\text{Geometric surface}}$$

The roughness factor is non-dimensional parameter, which is always greater than unit. Thus as $r$ increased, the total surface/interface energy increased gradually due to the increase in the actual area. It has been incorporated directly into the Wenzel model and plays an amplified role in wetting properties. But the Wenzel state prevails when the surface is completely wetted, i.e., homogeneous wetting as shown in Fig. 3A.

It is evident that a rough surface provides an additional interfacial area for the spreading liquid, thus the true CA would be different than the nominal CA. The additional surface area provided by roughening the surface results in the increase of surface energy. The effect of surface roughness on the equilibrium CA has been studied and an equation that gives a relation between equilibrium CA and the apparent angle formed on a rough surface has been proposed[27]:

$$\cos \theta_W = \text{r} \cos \theta_0 \qquad \ldots(7)$$

Where, $\theta_0$ is the equilibrium CA, $\theta_W$ is the apparent CA on a rough surface (generally known as

Wenzel angle) and r is the average roughness ratio. Hence r is the ratio of actual wetted surface area to geometric surface area calculated from radius of wetted base

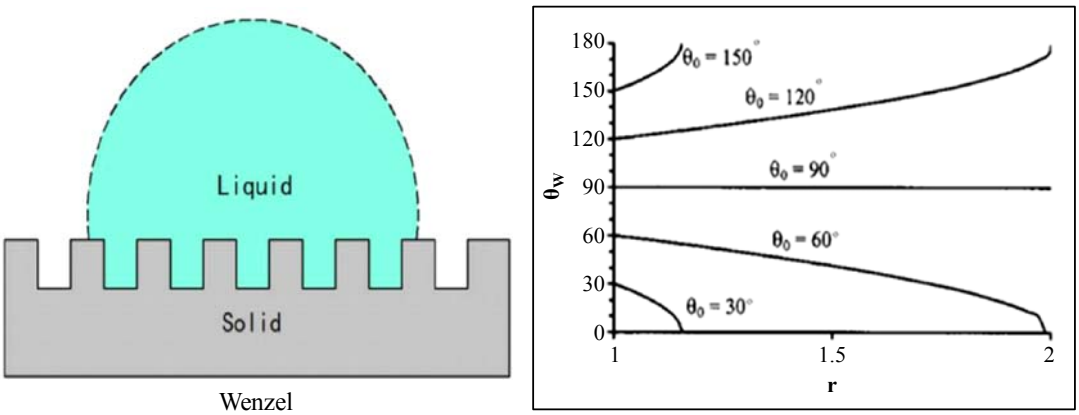


**Fig. 3: (a) Schematic diagrams of liquid droplets on micro-structured surfaces under the homogeneous (Wenzel) regime; (b) Contact angle ($\theta_W$) as a function of the roughness factor ($r$) for various CAs for smooth surface ($\theta_0$)**[17]

Wenzel's equation directly suggests that if $\theta_0 < \pi/2$ then $\theta_W < \theta_0$ and hence in this case the introduction of roughness will enhance the tendency for liquid to wet further. On the other hand, if $\theta_0 > \pi/2$ then $\theta_W > \theta_0$, the non-wetting tendency will be enhanced as shown in Fig. 3a. Thus in Wenzel's model, the roughness can amplify the wetting property of the solid surface if the liquid is initially wetting on smooth surface, resulting in more hydrophilicity. But if the liquid is non-wetting on the smooth surface early, then the introduction of the roughness can further make the surface of the solid substrate non-wetting, leading to the enhancement of hydrophobicity[28].

Compared to the Yong's equation, the Wenzel equation extends the smooth contact surface into a rough one, which induces a new realization for the mechanism of the surface wetting behavior.

Moreover, it introduces the concept of surface roughness, which makes the researchers realize the significance of the surface texture to the surface wettability. It has been demonstrated that surface roughness even plays a more important role than chemical compositions with low surface energy with regard to the superhydrophobic surfaces. However, it should be noted that the Wenzel equation should be confined in the thermodynamics stable equilibrium state. Usually, the energy barrier is often needed to be surmounted during the spreading of the liquid due to the heterogeneous of rough surfaces. If the vibrational energy is less than the energy barrier, the liquid will maintain a metastable state instead of stable state.

Wenzel equation[20] has revealed the relationship between the equilibrium CA and the apparent CA on a rough surface, but it is not valid while the solid surface is porous or composed of diffident chemical composition. For more careful consideration of these and several other details several other models, such as Cassie-Baxter model[21], composite structure with double-scale cylindrical groove model[22], a model with paraboloids of revolution[23] have been developed. The comprehensive overview of all these models is presented in paper[17].

## Hydrophobic surfaces for anti-stain coatings

Anti-staining is the ability to resist stains or easily erase the stains on the coated substrate[3,8,29,30]. This could be achieved by using low surface energy starting materials. On the other hand, the stability of the

coated substrate is also important criteria for creating stable properties. The stable substrate by using PMHS with 2,2,3,4,4,4 hexafluorobutylmethacrylate (HFBMA) and tetraethoxysilane (TEOS) *via* a sol-gel reaction have been prepared[3,14]. The spin coated PMHS (cured at 150°C for 24 h) showed a fractured surface morphology. On the other hand, the surface morphology of the PMHS was altered by the addition of HFBMA and TEOS. A smooth layered surface showed aggregated silica particle surface by increasing the TEOS content. The presence of micro/nanosilica particles on the fluorinated polymethylsiloxane/silica (FPMS/silica) hybrid showed hydrophobic properties[3,14]. The maximum roughness of the silica particles was ~27-35 nm, which depends on the concentration of TEOS content in the FPMS/silica hybrid surface.

The mechanical hardness or scratch resistance of the coated substrate was checked by a pencil hardness tester. The spin coated organic-inorganic hybrid material showed good scratch resistance (≥ 4H)[3]. Meanwhile, the scratch resistance of the substrate was altered by changing the concentration of ethanol[3,14]. Increasing the concentration of ethanol would lead to enhance the scratch resistance (≥ 5H) of the hybrid substrate[3,14]. The enhanced scratch resistance is due to the presence of hexagonally packed low surface energy fluorine atom on the outer surface which is bounded strongly on the substrate by silica particles.

Anti-staining property was checked by using water and oil based pens by simply writing and erasing on the coated substrate[3,8,14]. The FPMS/silica hybrid material showed good erasing property for both oil and water based pens for over 8 times by wiper paper[3,14]. The obtained results explain that the low surface energy matrix with good adhesive property is responsible for developing anti-stain coating. Transparency of the substrate is another important criterion for coating application. The FPMS/silica hybrid material showed 95% to 98% transparency in the visible region[3,14]. To enhance the anti-stain properties for practical applications, a novel metallopolymer hybrid material using PVC as a starting material has been developed[8]. A pre-synthesized iron-mercapto complex was grafted with PVC and then modified with mercapto silane precursor.

The authors will not go into detailed description of the FPMS-based hybrid materials because they are beyond the frame of current overview.

The PVC metallopolymer showed very good hydrophobicity with CA ~143.27° ± 2.0°.[8] PVC has good transparency (98% at 400 nm wavelength) in the visible region (Fig. 4a-c). The poly (vinyl chloride-g-ferrotrimethylolpropane tris(3-thiopropionate)) (PVCFeS) metallopolymer also maintains the transparency by drying up to 80°C for less than 24 h (Fig. 4d-f). On the other hand, the transparency of the substrate was decreased by further increasing the drying temperature to 150°C (Fig. 4g-k). Mercapto silane precursor and methyl silane precursor were introduced separately into the PVCFeS metallopolymer (mercapto silica functionalized PVCFeS (PVCFeS-SiSH), and methylsilica functionalized PVCFeS (PVCFeS-SiMe) in order to enhance the transparency (Fig. 4l and m)[8]. The hybrid metallopolymer maintained the transparency and enhances scratch resistance and anti-stain properties even by increasing the drying temperature to 150°C. This is due to higher boiling point of the mercapto silane precursor, which maintains the coloration of metallopolymer and enhances other properties. PVC metallopolymer hybrid showed improved scratch resistance (> 8H) and anti-staining properties (more than 10 times of writing and erasing test) as compared to the hybrid material surface made from PMHS[3,8,14].

Due to excellent lubrication of PVC metallopolymer hybrid substrate, the surface can easily drag away the water droplet at the sliding angle. This can lead to the use of the surface in self-cleaning coatings for practical applications. The self-cleaning properties of the PVC metallopolymer hybrid substrate was checked by spreading activated charcoal powder on the surface followed by dropping water droplets on the substrate. The bare glass showed the adhesion of charcoal on the substrate. On the other hand, the adhesion property was reduced on the PVC metallopolymer and their hybrid substrate. This proved the excellent anti-stain property of the PVC metallopolymer hybrid[8].

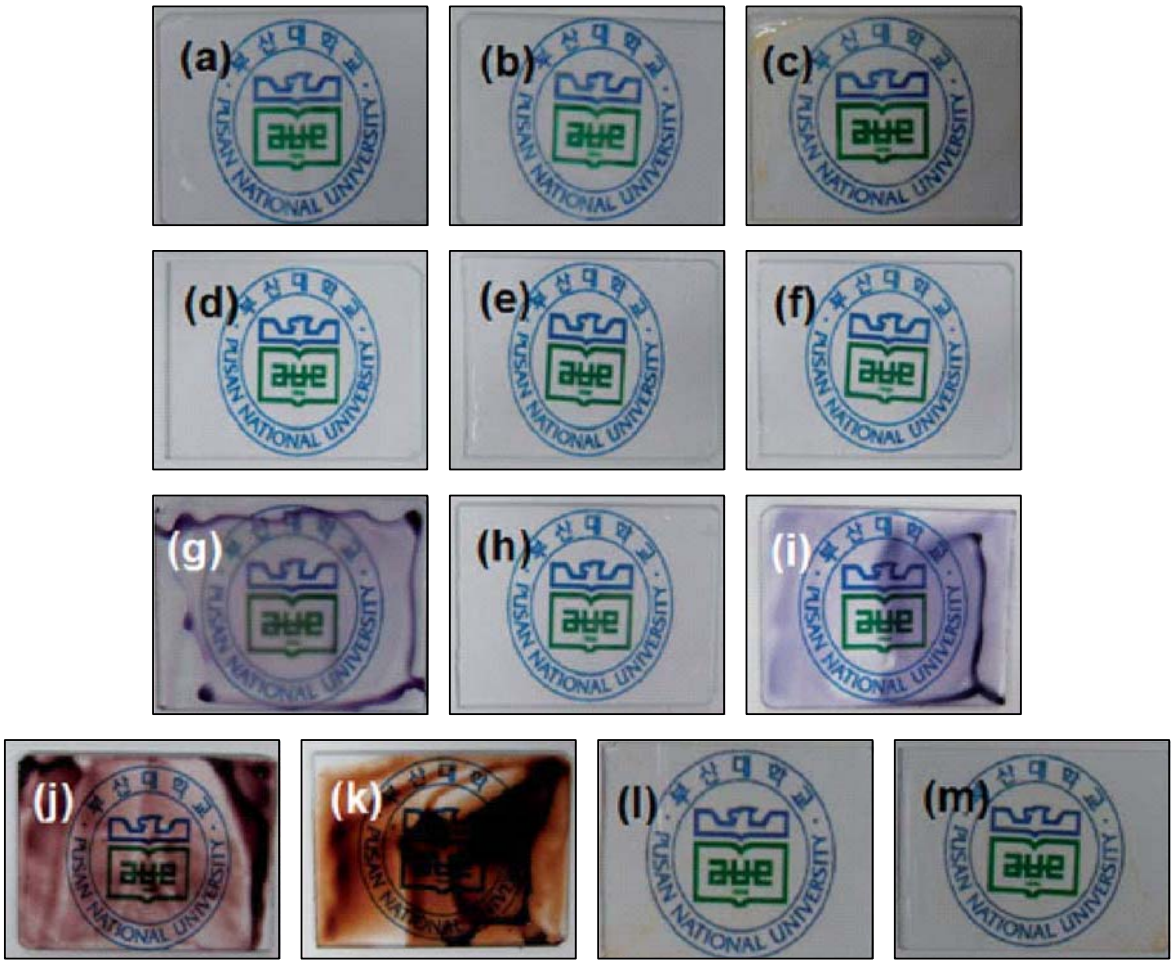


**Fig. 4: (a–c) Optical images of the spin coated poly(vinyl chloride) (PVC) substrate cured at room temperature, 80°C, and 150°C for 24 h. (d–f) poly(vinyl chloride-g-ferrotrimethylolpropane tris(3-thiopropionate)) (PVCFeS) metallopolymer substrates cured at room temperature, 40°C, 80°C for 1 h, (g) 80°C for 24 h, (h and i) 100°C for 1 h and 7 h, (j) 120°C for 1 h and (k) 150°C for 30 min. (l and m) Mercaptosilica functionalized PVCFeS (PVCFeS-SiSH), and methylsilica functionalized PVCFeS (PVCFeS-SiMe) metallopolymer substrates cured at 150°C for 24 h[8]**

## Superhydrophobic surfaces for non-stick and self cleaning applications

Non-stick and self-cleaning properties are depending on the sliding angle of the substrate surface. The free rotation and displacement of water droplets on the substrate surface can exhibit excellent self-cleaning behavior[9,13,16,31]. The non-stick property was tested on the superhydrophobic hybrid substrate by a water droplet (surface energy of water, 72 (mN/m)) or from the movements of water droplets on the substrate. Due to very high CA of the hybrid substrate can easily resist water droplets on the substrate. Superhydrophobic substrate can also easily drag away the water droplets and keep the substrate clean. This self-cleaning behavior was checked further by placing various dusts (zinc dust (< 10 μm), Portland cement, sea sand and carbon dust) on the drop coated or spin coated substrate followed by dropping water droplets[13,16,29]. The pollutants were collected by the droplets and drag away from the substrate (Fig. 5). This self-cleaning lotus leaf behavior was also achieved from the lotus leaf powder hybrid micro-nanocomposites. Similarly, Xu et al. fabricated superhydrophobic self-cleaning surface using titanium dioxide ($TiO_2$)/high density polyethylene (HDPE)[29].

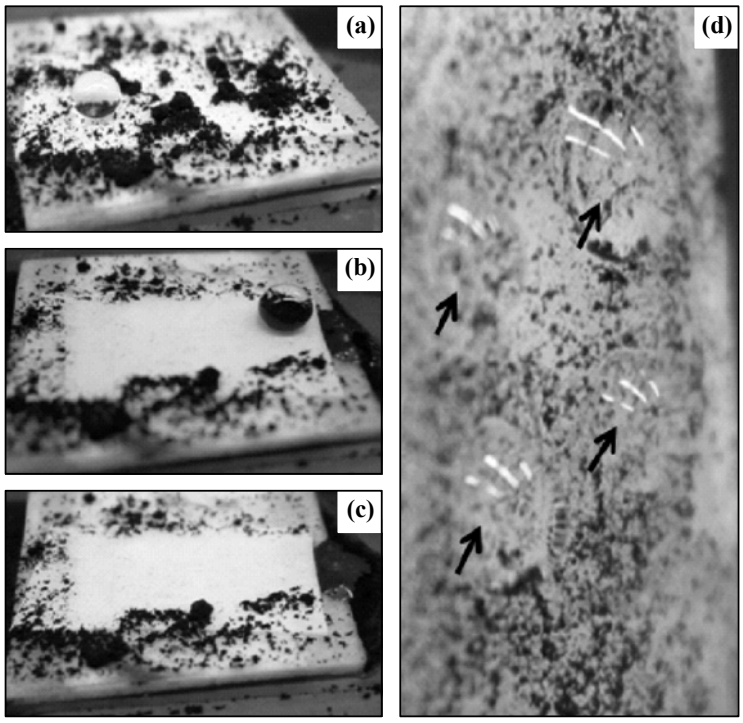


**Fig. 5: The self-cleaning effect of water droplets on the $TiO_2$-HDPE composite superhydrophobic surface (a-c), and sticky water droplets (marked) on a normal flat HDPE surface put vertically (d) The black contaminates are fine carbon particulates with an average size of 1 µm[29]**

$TiO_2$ in the HDPE have enhanced the self-cleaning properties of the substrate due to photo-oxidation of $TiO_2$ in UV light[29]. The stability of the bio-inspired hybrid micro-nanocomposites was also checked by varying the compositions of the starting materials[9,16,31].

According to[9], the superhydrophobic surfaces can be prepared in three ways, top-down, bottom-up and combination of top-down and bottom-up approaches[10]. In most cases, a superhydrophobic surface is prepared mainly by a combination of micro–nanostructures and enhancement of the roughness, surface area and air trapped in the rough surface[30,32]. This can create higher roughness and produce a hierarchical surface at the substrate. This hierarchical surface can have a higher equilibrium CA and show a transition from the Wenzel to Cassie–Baxter state[17,18,33-35].

Lotus leaves exhibit this combination of a micro–nano-hierarchical surface, and is a well known example of a superhydrophobic surface with a CA higher than 150$^o$ (Fig. 6a). The leaf surface also exhibits superoleophilic properties for dodecane oil (surface tension, 25.38 mN/ m, Fig. 6b).

When an oil drop (hydrocarbon oil) comes in contact with the leaf surface, the surface roughness at the leaf can increase the oleophilicity and introduce superoleophilicity due to the low surface-energy of the micro–nanocomposite.

**Note**: Superhydrophobic poly(methylhydroxysiloxane), PMHOS was prepared from PMHS (4.7 g, 78 mmol MeHSiO) was dissolved in anhydrous ethanol (70 mL) in a 100 mL glass container, followed by the addition of sodium hydroxide (0.008 g, 0.2 mmol in 2 mL of water) solution with constant stirring for 24 h.26 Hydrolyzed gel was obtained at room temperature in 24 h and dried completely at 80$^o$C for 24 h. The dried product was ground into a powder, washed several times in deionized water and vacuum dried overnight at 80$^o$C followed by further grinding into a fine powder. Preparation of instant superhydrophobic

hybrid micro–nanocomposites (LLPPSiOr) LL powder (0.05 g), PMHOS (0.25 g), ethanol (8 g, 173.7 mmol), and deionized water (1 g, 55.5 mmol) were placed into a glass container (30 mL) and stirred well for 1 h. The mixture of LL powder and PMHOS was called LLP. PSiOr suspension (0.1 g) was added to the LLP suspension, and the container was closed and stirred at room temperature for 24 h. The obtained hybrid suspension, which was called LLPPSiOr, was further ultrasonicated for 2 min.

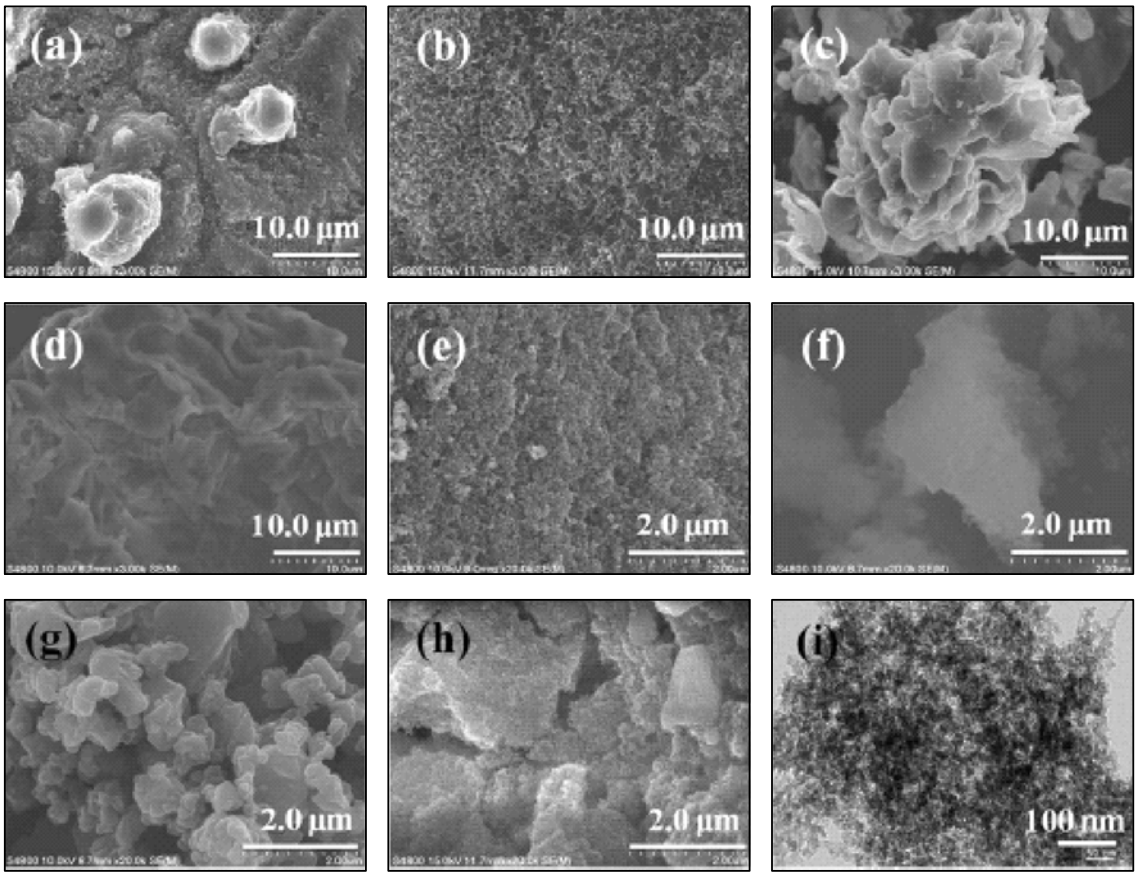


**Fig. 6: High resolution scanning electron microscopy HRSEM images of (a and b) LL at the front and rear surfaces, (c) LL powder, (d–f) LL powder, PMHOS and LLP dispersed in ethanol and cast on a glass substrate. (g) PSiOr dispersed in methanol. (h) LLPPSiOr hybrid micro nanocomposites dispersed in ethanol/methanol. (i) HRTEM image of LLPPSiOr hybrid micro-nanocomposite powder dispersed in ethanol by sonication for 10 min**[9]

The introduction of lotus leaf powder prepared at various drying temperatures (LL25°C, LL50°C and LL100°C) or hydrophilic silica nanoparticles (SiNPs) to the hybrid suspension (LL powder, PMHOS, and SiNPs (LLPSiNPs) hybrid micro-nanocomposites) showed stable hydrophobicity with spherical shape particles on the substrate[16]. Increasing the hydrophilic silica nanoparticles to the hybrid suspension also maintained the hydrophobicity on the coated substrate. The authors of paper[30] also prepared the bio-inspired hybrid micro nanocomposites using another leaf powder such as tree leaf powder (TL) powder. The TL powder showed better compatibility with the superhydrophobic PMHOS. The addition of hydrophobic PSiOr to the TLP suspension (TL powder and PMHOS in ethanol) also produced superhydrophobicity on any substrates. The surface property of the hybrid was tested at various temperatures of water droplets. The hybrid suspension maintains the superhydrophobicity to cold and hot water. The addition of water droplet at $0^{o}$C or below 0°C maintains the superhydrophobicity with stable contact angle as obtained for water droplet at room temperature.

The obtained results show the anti-icing property of the substrate. The superhydrophobicity was maintained on the substrate by placing water droplet temperature up to 50°C. Further increasing the water droplets temperature to 60°C to 80°C, the surface CA was reduced to hydrophobic by the nucleation of the hot water droplet on the substrate. Meanwhile, the superhydrophobicity can retain on the substrate by replacing the hot water droplet and placing the room temperature water droplet on the same place. The TL powder, PMHOS and PSiOr hybrid micro-nanocomposites (TLPPSiOr) also showed excellent non-stick and self-cleaning properties.

Superhydrophobic surfaces were also used in other applications such as cell adhesion and proliferation, drug delivery, organic dye loading and release, self-healing coatings, anti-corrosion, anti-fouling, and blood typing etc.[31,32].

**Scale up experience with polymer-based hybrid materials**

As it was mentioned in section 1, the organic-inorganic hybrid materials focused much attention in the recent days due to could be easily synthesized and produced in large scale[1].

As in was described in section 1, combination of organic polymers with hydrophobic nanoparticles has been studied extensively and there are hundred publications on the laboratory experience in the field of manufacturing such materials. However, relatively recent overview[2] provided several examples of scale up experience in this area.

For instance, aerogel/polymer –based organic–inorganic (O–I) nanocomposites can be considered as one of such examples. Despite the amazing intrinsic characteristics and properties of aerogels, most as-made aerogels present poor mechanical behavior: they are often highly brittle and fragile. This represents a serious drawback for their commercial applications. O–I hybridization of aerogels overcomes this lack of mechanical properties. Several strategies have been developed resulting in an increase in mechanical properties and facilitating then their further handling[2,36,37].

One of these strategies is based on the co-condensation of a flexible polydimethylsiloxane (PDMS) with TEOS. Gels obtained present a rubber-like flexibility and with 20% of PDMS, they can be elastically compressed by 30%[38]. Such mechanical properties (highly compressibility and elasticity) were also reached with aerogels synthesized with methyltrimethoxysilane as a unique precursor displaying compression capability between 60 and 80%[39,40]. This behavior was attributed to three factors provided by this hybrid network. First, with an organically substituted trialkoxysilane, the resulting network presents a lower crosslinking density making the macroscopic gel more flexible than bare silica. Second, the low density of silanol groups hinders the nonreversible shrinkage. Third, methyl groups are homogeneously distributed with high density in the network, which will repel each other during the temporal shrinkage on compression. In addition to the improvement of mechanical properties, these aerogels are highly hydrophobic (CA > 160$^{o}$), which is the main area of interest for current challenge.

Another interesting way of enhancing the mechanical properties of aerogels consists of the doping/reinforcing of aerogels by crosslinking organic polymers on the original gel skeletons. Based on the observation that polymers could be reinforced by inorganic fillers, the authors of studies[41-43] successfully increased the mechanical properties of aerogels by doping fillers (i.e. aerogels) with polymers. Briefly using pure silica gel[41] or amino-modified silica wet gel[42,43] (with 3-aminopropyltriethoxysilane as a co-precursor), polymerization was performed with diisocyanates[41], multifunctional epoxides[42] or p-chloromethylstyrene/ styrene[43] derivatives before the drying step.

However while the mechanical properties (strength, stiffness, flexibility) are usually enhanced by the organic polymerization, the insulating ability, optical transparency, and surface area are at the same time

reduced. It was possible, however, to increase the mechanical properties of aerogels and therefore to move to a commercial development is based on another type of reinforcement[2]. Like steel bars reinforce concrete in buildings, aerogels could be reinforced by microfibers. Using this approach, Aspen Aerogels, Inc started to fabricate in the early 2000's flexible fiber-hydrophobic silica aerogel composite blankets via a sol impregnation process followed by supercritical drying with $CO_2$. Depending on the formulation of composites (for example the type of fibers: organic or inorganic), aerogel-based insulation blankets were designed for cryogenic applications (Cryogels), for clothing and apparel (Pyrogels/Spacelofts) or for high-temperature applications (Pyrogels) allowing then insulation from - 265$^{o}$C to 650$^{o}$C.

Moreover, due to their low thickness, flexibility and easy handling features, they could easily insulate any type of plant's equipment (piping, towers, tanks, etc) even in confined spaces.

Their products are now found in subsea oil pipelines (pipe in pipe insulation), refineries, winter apparel (Fig. 7), building and construction. Considering the high optical transparency of aerogels in addition to their insulation properties (thermal and acoustic), Cabot Corporation incorporated its Nanogels granules in daylighting systems providing an enhancement of insulation while maintaining optimal light transmission. Aerogel granules/particles could be incorporated in many existing daylighting systems (structural composite panels, structural polycarbonate systems, U-channel glass, insulated glass units, etc).


**Fig. 7: Insulated apparel made of O–I nanocomposites: ''Hyper Elite/Uber Elite'' sleeping pads from Pacific Outdoor Equipment (Aspen Aerogel® products), ''Tundra'' winter boots/''F22W'' snowboard boots from Salomon (Aspen Aerogel® products), ''Quota Zero - EXTREME AEROGEL'' jacket from Grado Zero Espace: (Nanogelt$^{TM}$– Cabot Corporation®), ''Champion Supersuit'' from Hanesbrands Inc. (ZERO-LOFT$^{TM}$- Aspen Aerogel® - e21®), ''Nanogelite'' insulated bottle from Elite Srl (Nanogel$^{TM}$ – Cabot Corporation), ''Toasty Feet'' insulator insoles/''PolarPad'' seat pads from PolarWrap LLC: (Aspen Aerogel® products)[2]**

Considering commercial applications of hybrid polymer nanocomposites, the authors of overview[2] noticed that keeping in mind the extensive variety of both nano-objects which are mostly commercially

available (oxide-based particles, oxo-clusters, POSS, clays, nanoMOFs, metals, quantum dots, carbon nanotubes) and existing polymers, their potential combinations and thus the synergetic properties of the resulting nanocomposites are essentially endless. In many cases, the polymer matrix allows easy shaping and better processing of the materials. The inorganic components provide mainly mechanical and thermal stability, but also new functionalities that depend on the chemical nature, the structure, the size, the shape and crystallinity of the inorganic phase[44].

The inorganic component can implement or improve electronic, magnetic and redox properties, density, refraction index, etc. Obviously, the final materials are not only the sum of the primary components but a large synergy effect is expected from the close coexistence of the two phases through size domain effects and nature of the interfaces. Generally, the major features of each phase are preserved or even improved in the O–I nanocomposites (stability, mechanical and thermal behavior, specific properties, hydrophobicity, etc.), and furthermore, new properties coming from the synergy of both components are commonly observed as well[2].

It is worth mentioning that low-volume additions (1-10%) of nano-objects provide mechanical properties (like elastic stiffness and strength) enhancements with respect to the neat polymer that are comparable to that achieved by conventional loadings (15-40%) of traditional micrometer-scale inorganic fillers. This is generally explained by the large surface area to volume ratio of nano-objects when compared to the micro and macro-additives. In addition to that the lower particle loading facilitates processing and reduces component weight.

According to paper[2], commercial developments of the O–I nanocomposites s involve mainly two types of nano-objects: oxide-based particles (silica-based particles most of the time) and clays. This could be easily explained by the commercial availability and the relatively low cost of such nano-objects. Several strategies have been investigated to prepare these nanocomposites depending on the starting states of both organic and inorganic materials. The polymer matrix could be formed from molecular precursors (monomer – oligomer), preformed linear polymer (in molten, solution, or emulsion states) or a polymer network already cross-linked. Nano-objects could be introduced in the organic part either as molecular precursors or under preformed nano-objects. In practice, the majority of commercial developments involve preformed nano-objects. These nanoobjects could be incorporated in the polymer matrix by (i) melt processing (direct mixing of nano-objects with the polymer melt), by (ii) solution processing (a common solvent is used to disperse nano-objects in a polymer solution), by (iii) an in situ polymerization (dispersion of nanoparticles directly in the monomer or monomer solution).

Since mechanical and physical properties of the O–I nanocomposites depend directly on the uniform dispersion of nanofillers inside the polymer matrices, a surface-modification step is usually necessary to achieve high dispersion rates. Functionalization of these nano-objects requires molecules able to both bond to the particles surface and to interact with the polymer matrix. They should then present anchoring groups interacting with the inorganic particles through covalent, coordinative, electrostatic or hydrogen bonding and an organic part capable of forming covalent bonds (through a polymerization process) to the polymer matrix or interacting via van der Waals forces. Numerous compounds could be used for organically modifying the surface of nanoobjects, among them are silane coupling agents, complexing/ chelating agents, surfactants, block copolymers, organic ammonium/phosphonium cations[45-51].

According to authors of review[2], there is a strong wave of scientific and social thought and determination seeking a harmonization between nature and human ingenuity. In this vein, materials and systems created by humans must become increasingly recyclable, environmentally friendly, energy efficient, reliable, and inexpensive. New green strategies to process hybrids in water using natural polymers and COV-free media are already being investigated at the academic level. In this very active context, the

emergence of the hybrid world within the domain of smart materials has already begun and its continued growth seems assured due to a number of easily identifiable factors. As an example can be mentioned the economic and technical limitations, which always crop up in current technology and which are contrasted by the inexhaustible abundance of hybrid structures with a near infinite continuum of properties.

At the same time, predictive approaches to guide our knowledge of the material landscape and tame this abundance will become more accessible due to the bridging of the chemical and physical disciplines, a trend that is now expanding to biology. These predictive approaches are strongly associated to the development of more systematic fundamental studies that will allow the characterization of structure and dynamics of the hybrid interfaces or render it possible through monitoring and characterization in real time all the formation steps from molecular precursors to the final materials. Such experiments are of paramount importance as they will lead to the complete knowledge and control of these complex materials for which the resultant optimized properties arise from efficient chemistry processed coupling. This will allow predictive approaches to molecular engineering enabling hybrid materials to obtain full maturity, thus facilitating a more extended development at a larger industrial scale.

As an example of the industrial approach for treatment of the synthetic fabric (nylon, polyester, etc.) it seems to be appropriate to mention the technology of Shin Etsu Corporation[52,53]. This company has developed and commercialized the process of manufacturing oil-in-water emulsions consisting of dimethylsilicone or modified silicone emulsified with various emulsifiers. Silicones are chemically inactive, have very low surface tension and provide good water repellency, releasability, and lubrication. Thus, silicones are also commonly used as fiber and fabric processing agents. They are used to treat synthetic fabrics made of polyesters and polyamides to make them water repellent or waterproof, to impart flexibility, and are commonly used to improve the texture and sew ability of textile goods, resulting in higher grade and more functional products.

Besides forming a coating (oil film or hard coating) on textiles to provide excellent water repellency, silicone greatly reduces the friction coefficient between fibers to achieve distinctive softness. The flexible film which forms on the fiber surface improves the durability of the fabric with respect to washing and dry cleaning. Fabrics have excellent rebound resiliency ("stretch-back") due to the flexible elastic coating which forms on the fiber surface. Silicone processing agents improve the hyperchromic effect and colorfastness due to the transparent coating which forms on the fiber surface. The chemical bonds which form the backbone are siloxane bonds (Si-O-Si), so the interatomic bonding energy of these processing agents is high and they have excellent weather and heat resistance.

Besides oil-in-water emulsions Shin Etsu developed the solvent based water repellents.

Table 1 shows the general information related to properties of two solvent based water repellents which contain reactive silicones diluted with an organic solvent. Unlike emulsion type water repellents, solvent based reagents exhibit none of the negative effects associated with emulsifiers, and because organic solvents permeate easily into the fibers, the water repellency treatment is highly effective.

Referring to Table 1, KS-7001 is one-component, room-temperature water repellent. It performs well with polyamide and polyester fabrics providing a soft ans silky wet texture. Another product, POLONCOAT-E provides highly durable waterproofing, These water repellent can be used fot anti-melt treatment of synthetic fibers, and for treating fabrics to enhance rebound resilience.

Thechnical bulletin[52] provides some detais of the treatments procedures for fabrics made of synthetic fibers. It is indicated that if the fabric is to be treated for water repellency, it is necessary to scour the raw fabric. Hydrofilic sizing agents, surfactants, oil solutions and other substances remain when the textile is

treated with silicon, it will be difficult to achieve good water repellency, and the treatment will be less durable against repeated washes.

**Table 1: Two types of solvent based water repellents manufactured by Shin Etsu corporation**[52]

| Parameter / Grade | Appearance | Viscosity mPa·s | Nonvolatile content (%) (105°C × 3 h) | Specific gravity (25°C) | Solvent | Catalysts with which softener are typically used |
|---|---|---|---|---|---|---|
| KS-7001 | Colorless transparent liquid | 7 | 21 | 0.8 | Isopropyl alcohol | Self crosslinking |
| Polancoat-E | Colorless to pale yellow transparent liquid | 15,000 | 27 | 0.9 | Toluene | CAT-PG, CAT-PD |

(Not specified values)

In order to make the treatment more effective several catalysts have been developed[52] (Table 2). It sould be mentioned, however, that in general, the user may experience problems with silicone textile treatments if the main agent and catalyst are mixed together directly. With emulsion products, this can mean gelation or separation: with solution type products, it can lead to thickening or reduced stability of the treatment bath. Therefore it is critical to delute the components before mixing. Besides in was noted[52] that the method of preparing the treatment solution differs from product to product, it is important to be sure to use a method that works for particular product.

**Table 2: Two type of catalysts recommended for application of the solvent-based water repellents**[52]

Catalysts for use with solution type silicone textile treatments

| Parameter / Grade | Features | Appearance | Non-volatile matter content (%) (105°C × 3 h) | Standard blend ratios* (%) | Applicable textile treatments |
|---|---|---|---|---|---|
| CAT-PG | Catalyst for water proof coating agents<br>Toluene solution.<br>High activity | Colorless to pale yellow transparent liquid | 43 | 2-5 | Poloncoat-E |
| CAT-PD | Adhesion assistant<br>Reaction promoter<br>Ethanol solution | Colorless to pale yellow transparent liquid | 10*2 | 2-5 | |

*1: Standard blend ratios are indicated as X parts by weight to 100 parts of the main agent.

*2: Amount of active ingredient (due to low boiling point of main ingredients)

(Not specified values)

As for type of application procedure, the dipping, coating, or coating may be used. The tubs made of stainless steel which should be cleaned thoroughly prior to appliction, are strongly recommended. The bath temperature should be kept below 30°C to prevent degradation of the treatment solution.

In general fabrics should first be dried to remove moisture or solvent in preparation for heat treatment. The treatment conditions will vary depending on various factors including the type of fiber, close thickness, the resin used in combination, and the dryer used. But as a general rule, baking equipment or heat setting equipment capable of heating to 140-180°C should be used (Table 3).

**Table 3: Preparatory drying and heat treatment temperatures**[52]

| Textile treatment agent | Preparatory drying temp. ($^oC$) | Heat treatment temp. ($^oC$) |
|---|---|---|
| Polon-MR | 80-100 | 130-150 |
| Polon-MF-23 | | |
| Polon-MK-206 | 80-100 | 130-160 |
| Poloncoat-E | 50-80 | 120-180 |

• Times required for preparatory drying and heat treatment will vary depending on the condition of the textile being processed, but in most cases the following will serve as general guidelines.

Preparatory drying: 80-100°C/2-5 min. Heat treatment: 120-180°C/1 -5 min.

If the textile is treated with silicon alone, there is generally no need for soaping or a warm water wash afterward. However, when emulsion type silicon textile treatments are used in combination with resin treatment agents, the fabric should be soaped or washed in warm water to remove unreacted resins, surfactants or other unwanted substances to boost the water repellency effect and to remove odors.

Considering different methods of treatment for polyester fabric, it is necessary to mention the procedure for making O-I nanocomposite containing nanoparticles of titanium dioxide[54]. Nano-$TiO_2$ sol and finishing agent was prepared by sol-gel method, during which tetrabutyl titanate was used as precursor and ethanol was used as solvent. The agent was penetrated into polyester fabric through a padding method, the anti-ultraviolet performance of the fabric was analyzed and the external morphology was carefully studied afterward. The results showed that indicated that the Nano- $TiO_2$ particles distribute evenly with fine dispersity (Fig. 8) and stability and the finished fabrics demonstrated exceptional anti-ultraviolet performance.

Fig. 8a and 8b are the fiber surface topography after 1000 times of magnification. By comparing the two images, we can see that the unfinished fiber surface is smooth and sleek while the finished has deposited Nano-$TiO_2$ on the fiber surface ranging in an inconsecutive way with some aggregation formed due to the minimal-particle-size-led self-aggregating phenomenon of Nano- $TiO_2$. Consecutive Nano- $TiO_2$ particles ranged in a dispersed way leading to an irregular surface.

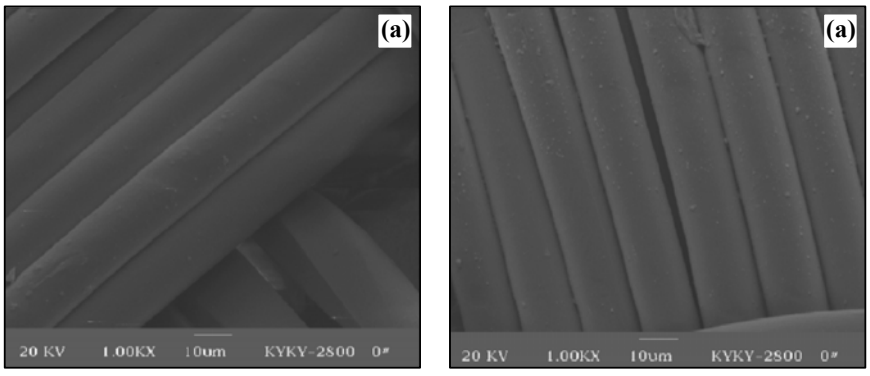


**Fig. 8: SEM images of the surface distribution of polyester fabrics: (a) unfinished fabric; (b) finished fabric**[54]

The following procedure has been used for preparation of nanoparticles of titanium dioxide. Add certain quantity of tetrabutyl titanate precursor into the anhydrous ethanol with a 1:10 ratio, sufficient stir to

get a fully resolved mixed solution A. Next put the catalyst $HNO_3$ into distilled water to make mixed solution B and then add A into B drop by drop under quick stirring state. Maintain that state under room temperature for a certain length of time and the uniformly distributed transparent Nano-$TiO_2$ sol could be prepared.

The chemistry of the sol-gel process can be represented as follows:

It is well-documented that titanium alkoxide react with water through the reactions shown in Eqs. (8) (9) (10) and (11).

Hydrolysis:

$$Ti\ (OR)_n + H_2O \rightarrow Ti(OH)(OR)_{n-1} + ROH \quad \ldots(8)$$

$$Ti\ (OR)_{n-1} + H_2O \rightarrow Ti(OH)_2(OR)_{n-2} + ROH \quad \ldots(9)$$

Condensation:

$$-Ti\text{-}OH + HO\text{-}Ti \rightarrow -Ti\text{-}O\text{-}Ti + H_2O \quad \ldots(10)$$

$$-Ti\text{-}OR + HO\text{-}Ti \rightarrow -Ti\text{-}O\text{-}Ti + ROH \quad \ldots(11)$$

The Finishing process: The polyester fabric processed by plasma ion gas with power of 100KW, processing time of 10 min, then dipping the fabric into the Nano-$TiO_2$ sol, at 60°C, processing time of 40 min, then dry out under 80°C.

Slightly different approach for producing polyester fabric treated with nanoparticles of - $TiO_2$ and $SiO_2$ was reported in study[55]. The authors of this study have developed a simple, but very effective and versatile, method to produce an imbalanced surface tension across the thickness of fabrics, and demonstrated that the fabrics have the ability to spontaneously transfer water unidirectionally through the fibrous architecture. A plain weave polyester fabric (thickness 520 mm) has been used as a sample porous membrane.

The proposed method is based on a solution coating technology to form a superhydrophobic layer containing $TiO_2$ and hybrid silica on a polyester fabric, and subsequent exposure of the one side of the superhydrophobic fabric to a multi-wavelength UV-beam to make the irradiated fabric side hydrophilic, leading to the formation of asymmetric wettability through the fabric thickness.

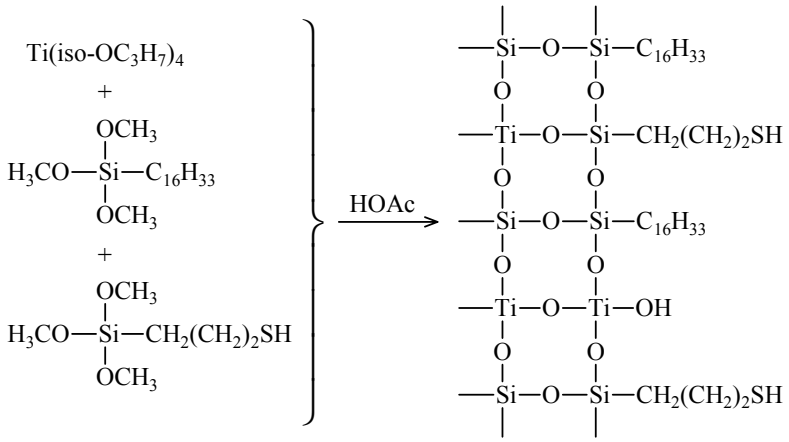


**Fig. 9: The superhydrophobic coating formation**[55]

The coating solution was prepared by a sol–gel route similar to the synthesis of $TiO_2/SiO_2$ hybrid materials from titanium tetraisopropoxide and tetraethylorthosilicate[56] but different in that two organic silanes (hexadecyltrimethoxysilane and 3-trimethoxysilylpropanethiol-1) (Fig. 9) were used to leave non-hydrolysable groups in the product.

Through a dip-coating process, a thin layer of conformal coating composed of $TiO_2$ and hybrid silica having hydrophobic hexadecyl and 3-thiol propyl groups was readily formed through the polyester fabric. Fig. 10 (Right panel) shows the scanning electron microscopic energy-dispersive X-ray (SEM-EDX) mapping images, indicating the formation of a uniform coating layer. The surface water contact angle increased to 170$^o$ on both sides of the fabric after the coating formation (Left panel of Fig. 10).

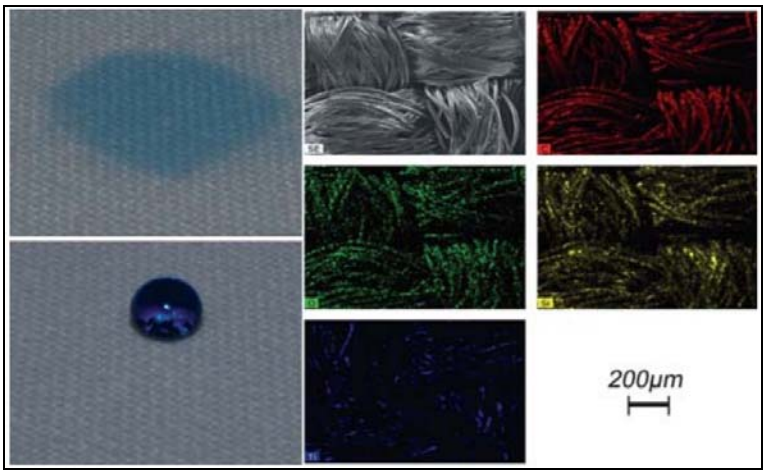


**Fig. 10: Digital photographic images of water spreading in the plain weave polyester fabric (Top left) and forming a water droplet on the $TiO_2$-silica coated polyester fabric (Bottom left), and SEM-EDX mapping of element C, O, Si, S and Ti on the coated fabric (Right panel)**[55]

Subsequent UV irradiation from one side of the fabric led to a series of chemical reactions catalysed by $TiO_2$ within the irradiated portion of the membrane[56,57] converting those pre-formed hydrophobic surface groups in the coating layer into hydrophilic oxygen containing groups, including the highly water-absorptive sulfonic acid and carboxylic acid.

The authors will not go to details related to making the coated fabric hydrophilic because it is outside of the purpose of the current review. In contrary, it seems to be appropriate to find an easy practical way to maintain the level of hydrophobicity which has been reached, i.e CA~170$^o$ on both sides of the polyester fabric after coating (Fig. 9 and 10). One of such possibility is to use UV fabric protectors, like Ray Block UV Fabric protector commercially available from Trek7, Inc (Upland, CA)[58].

## CONCLUSION

In summary, the authors considered the theory of superhydrophobicity, as well as basic approaches to creation of hydrophobic surfaces for anti-stain coatings and superhydrophobic surfaces for non-stick and self cleaning application. The main aspects of scale up experience with polymer-based hybrid materials were analyzed and it was concluded that the fluorination-free method of increasing hydrophobicity of polyester and polyamide fibers has the highest potential in terms of practical needs. It was shown that the sol-gel process based on using titanium tetraisopropoxide and two organic silanes (hexadecyltrimethoxysilane and 3-trimethoxysilylpropanethiol-1, as starting materials appears to be most promising route to the industrial applications.

## REFERENCES


1. C. Sanchez, B. Julian, P. Belleville and M. Popall, J. Mater. Chem., **15**, 3559-3592 (2005).
2. C. Sanchez, P. Belleville, M. Popall and L. Nicole, Chem. Soc. Rev., **40**, 696-753 (2011).
3. S. Nagappan, M. C. Choi, G. Sung, S. S. Park, M. S. Moorthy, S. W. Chu, W. K. Lee and C.S. Ha, Macromol. Res., **21**, 669-680 (2013).
4. C. M. Hui, J. Pietrasik, M. Schmitt, C. Mahoney, J. Choi, M. R. Bockstaller and K. Matyjaszewski, Chem. Mater., **26**, 745-762 (2014).
5. J. Pyun and K. Matyjaszewski, Chem. Mater., **13**, 3436-3448 (2001).
6. Z. Yan, L. Ma, Y. Zhu, I. Lahiri, M. G. Hahm, Z. Liu, S. Yang, C. Xiang, W. Lu, Z. Peng, Z.Sun, C. Kittre, J. Lou, W. Choi, P. M. Ajayan and J. M. Tour, ACS Nano, 7, 58-64 (2013).
7. S. Pandey and S. B. Mishra, J. Sol-Gel Sci. Technol, **59**, 73-94 (2011).
8. S. Nagappan, S. S. Park, E.-J. Yu, H.-J. Cho, J. J. Park, W.-K. Lee and C.-S. Ha, J. Mater. Chem. A, **1**, 12144-12153 (2013).
9. S. Nagappan, J. J. Park, S. S. Park, W.-K. Lee and C.-S. Ha, J. Mater. Chem. A, **1**, 6761-6769 (2013).
10. X.-M. Li, D. Reinhoudt and M. Crego-Calama, Chem. Soc. Rev., **36**, 1350-1368 (2007).
11. M. Liu and L. Jiang, Adv. Funct. Mater., **20**, 3753-3764 (2010).
12. S. Nagappan and C. S. Ha, Austin. J. Chem. Eng., **1(1)**, 1003 (2014).
13. S. Nagappan, J. H. Park, A. R. Sung and C.-S. Ha, Compos Interfaces, **21**, 597-609 (2014).
14. S. Nagappan, J. J. Park, S. S. Park, S.-H. Hong, Y.S. Jeong, W.-K. Lee and C.-S. Ha, Compos Interfaces, **20**, 33-43 (2013).
15. E. Keinan and N. Greenspoon, J. Org. Chem., **48**, 3545-3548 (1983).
16. S. Nagappan, A. R. Sung and C.-S. Ha, J. Bio-based Mater. Bioenergy, **8**, 175-183 (2014).
17. B. Wang, Y. Zhang, L. Shi, J. Li and Z. Guo, J. Mater. Chem., **22**, 20112-20127 (2012).
18. T. Onda, S. Shibuichi, N. Satoh and K. Tsujii, Langmuir, **12**, 2125 (1996).
19. R. Blossey, Nature Mater., **2**, 301-306 (2003).
20. R. N. Wenzel, Ind. Eng. Chem., **28**, 988-994 (1936).
21. A. B. D. Cassie and S. Baxter, Trans. Faraday Soc., **40**, 546-551 (1944).
22. N. A. Patankar, Langmuir, **20**, 7097-7102 (2004).
23. A. Marmur, Langmuir, **20**, 3517-3519 (2004).
24. M. M. Schwartz and S. Aircraft, Metals hand Book, 10th Ed, Metals Park, OH: ASM, **6** (1991) pp. 126-129.
25. J. N. Israelachvili, Intermolecular and Surface Forces, 2nd Ed, Academic Press, London (1992).
26. M. Nosonovsky and B. Bhushan, Microsyst. Technol., **11**, 535-549 (2005).
27. A. W. Adamson and A. P. Gast, Physical Chemistry of Surfaces, 6th Ed, Wiley-Interscience, New York (1997) pp. 347-379.
28. B. He, J. Lee and N. A. Patankar, Colloids Surf. A, **248**, 101-104 (2004).

29. Q. F. Xu, Y. Liu, F.-J. Lin, B. Mondal and A. M. Lyons, ACS Appl. Mater. Interfaces, **5**, 8915-8924 (2013).
30. W. Barthlott and C. Neinhuis, Planta, **202**, 1-8 (1997).
31. S. Nagappan , S. S. Park and C. S. Ha, J. Nanosci. Nanotechnol., **14**, 1441-1462 (2014).
32. D. Quere, Nat. Mater., **1**, 14-20 (2002).
33. E. Bormashenko, Philos. Trans. R. Soc. A, **368**, 4695-4711 (2010).
34. G. Liu, L. Fu, A. V. Rode and V. S. J. Craig, Langmuir, **27(6)**, 2595-2600 (2011).
35. T. Onda, S. Shibuichi, N. Satoh and K. Tsujii, Langmuir, **12(9)**, 2125-2127 (1996).
36. A. C. Pierre and G. M. Pajonk, Chem. Rev., **102**, 4243-4265 (2002).
37. A. Soleimani Dorcheh and M.H. Abbasi, J. Mater. Process. Technol., **199(1-3)**, 10-26 (2008).
38. S. J. Kramer, F. Rubio-Alonso and J. D. Mackenzie. Mater. Res. Soc. Symp. Proc., **435**, 295-300 (1996).
39. K. Kanamori, M. Aizawa, K. Nakanishi and T. Hanada, Adv. Mater., **19(12)**, 1589-1593 (2007).
40. A. V. Rao, N. D. Hegde and H. Hirashima, J. Coll. Interface Sci., **305**, 124-132 (2007).
41. N. Leventis, C. Sotiriou-Leventis, G. Zhang and A.-M. M. Rawashdeh, Nano Lett., **2**, 957-960 (2002).
42. M. A. B. Meador, E. F. Fabrizio, F. Ilhan, A. Dass, G. Zhang, P. Vassilaras, J. C. Johnston and N. Leventis, Chem. Mater., **17**, 1085-1098 (2005).
43. F. Ilhan, E. F. Fabrizio, L. McCorkle, D. A. Scheiman, A. Dass, A. Palczer, M. A. B. Meador, J. C. Johnston and N. Leventis, J. Mater. Chem., **16**, 3046-3054 (2006).
44. F. Mammeri, E. Le Bourhis, L. Rozes and C. Sanchez, J. Mater. Chem., **15**, 3787-3811 (2005).
45. A. B. Morgan, Polym. Adv. Technol., **17**, 206-217 (2006).
46. R. A. Vaia and J. F. Maguire, Chem. Mater., **19**, 2736-2751 (2007).
47. H. Zou, S. Wu and J. Shen, Chem. Rev., **108**, 3893-3957 (2008).
48. B. Chen, J. R. G. Evans, H. C. Greenwell, P. Boulet, P. V. Coveney, A. A. Bowden and A. Whiting, Chem. Soc. Rev., **37**, 568-594 (2008).
49. H. Althues, J. Henle and S. Kaskel, Chem. Soc. Rev., **36**, 1454-1465 (2007).
50. E. P. Giannelis, Adv. Mater., **8(1)**, 29-35 (1996).
51. M. Alexandre and P. Dubois, Mater. Sci. Eng. R, **28**, 1-63 (2000).
52. Textile Treatments, Bulletin of Shin Etsu Corporation, www.shinetsusilicone-global.com/catalog/pdf/ TextileTreatments_e.pdf.
53. http://www.shinetsusilicone-global.com/products/type/fiber_processing/
54. H. Li, H. Deng and J. Zhao, Int. J. Chem., **1(1)**, 57-62 (2009).
55. H. Wang, J. Ding, L. Dai, X. Wang and T. Lin, J. Mater. Chem., **20**, 7938-7940 (2010).
56. J. K. Walters, J. S. Rigden, P. J. Dirken, M. E. Smith, W. S. Howells and R. J. Newport, Chem. Phys. Lett., **264**, 539-544 (1997).
57. C. Anderson and A. J. Bard, J. Phys. Chem., **99(24)**, 9882-9885 (1995).
58. Ray Block UV Fabric Protector, www.trek7.com